Metal–Organic Frameworks

DOI: 10.1002/anie.200903366

Local Vibrational Mechanism for Negative Thermal Expansion: A Combined Neutron Scattering and First-Principles Study**

Vanessa K. Peterson, Gordon J. Kearley, Yue Wu, Anibal Javier Ramirez-Cuesta, Ewout Kemner, and Cameron J. Kepert*

Metal–organic frameworks, in addition to being sufficiently robust to support substantial micropore volume and therefore display reversible host–guest chemistries,[1] are increasingly being appreciated for their rich structural flexibilities.[2–4] The under-constrained connectivities and low deformation energies of these materials manifest themselves both in their often marked static deformations with guest exchange[3] and in their dynamic deformations with the thermal population of low energy transverse vibrations.[4] Interest in the latter has seen the discovery of two broad new classes of negative thermal expansion (NTE) material, namely, metal cyanides[5] and metal–organic frameworks,[6,7] noteworthy due to their novel NTE mechanisms and pronounced NTE behaviors.

Among the metal–organic framework systems yet shown to display NTE, $[Cu_3(btc)_2]$ (also "HKUST-1";[8] btc = 1,3,5-benzenetricarboxylate), consisting of a cubic 3D framework of dinuclear $\{Cu_2(carboxylate)_4\}$ "paddlewheel" units bridged by btc, is of particular interest in providing two new vibrational mechanisms for NTE: transverse displacement of the pseudo-planar btc units (the first instance where 3- rather than 2-connecting bridges contribute to NTE) and twisting within the paddlewheel units (the first instance where local deformations are thought to contribute to NTE);[6] see insets to Figure 1. For the former, variable-temperature single crystal X-ray diffraction (SCXRD) analysis suggested two important low-energy btc modes: translation perpendicular to the plane and libration about axes within the plane, with these modes thought to be coupled through the concerted rotation of the dinuclear paddlewheels to give a broad spectrum of rigid unit modes; notably, some libration of the btc units is necessary to relieve frustration arising from the strained octahedral supramolecular subunits within the structure.[6] Here we explore the nature and relative importance of these mechanisms through a detailed investigation of the lattice dynamics, which shows that the low-energy paddlewheel motions are essentially localized.

To probe the low-temperature thermal expansion behavior we collected high-resolution neutron powder diffraction (NPD) data on a deuterated sample of $[Cu_3(btc)_2]$ over 20 to 300 K (see Figure 1). The data in the range 100 to 300 K gave

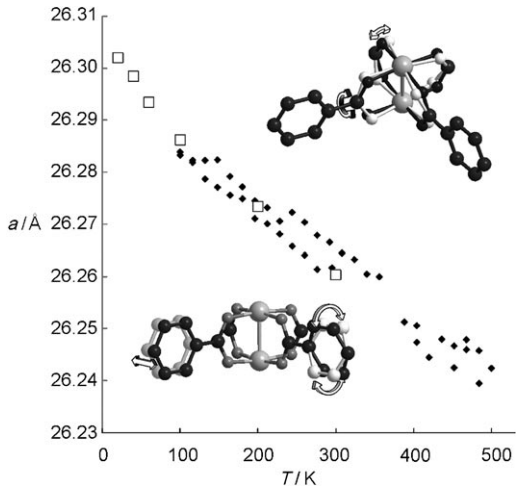

Figure 1. NTE behavior of $[Cu_3(btc)_2]$ obtained from NPD (□) and SCXRD (◆)[6] data, where *a* is the lattice parameter. The insets show the two proposed NTE mechanisms: paddlewheel deformation (upper right) and transverse btc displacement (lower left).

an NTE coefficient $\alpha_a = (\partial \ln a/\partial T)_p = -4.9(1) \times 10^{-6}\ K^{-1}$, consistent with that found for the protonated phase by X-ray diffraction (XRD).[6] Unusually, we find an increase in NTE at lower temperatures, with $\alpha_a = -7.5(3) \times 10^{-6}\ K^{-1}$ in the range 20 to 100 K. The temperature dependent structural models refined from these data are consistent with those determined by SCXRD at higher temperatures:[6] from 20 to 100 K the most rapid increase in isotropic atomic displacement parameters (ADPs) occurs for the carboxylate oxygen atom, and the largest negative rate of apparent bond-length change occurs for the Cu–O bond; both behaviors are consistent with that expected for thermal population of motions associated with the paddlewheel deformation (see Supporting Information).

Temperature-dependent inelastic neutron scattering (INS; neutron energy loss) data maintained features up to

[*] Dr. V. K. Peterson, Prof. G. J. Kearley
The Bragg Institute, Australian Nuclear Science and Technology Organisation, PMB1 Menai, NSW (Australia)
Fax: (+61) 29717-3606
E-mail: vanessa.peterson@ansto.gov.au
Y. Wu, Prof. C. J. Kepert
School of Chemistry, The University of Sydney (Australia)
Dr. E. Kemner
Berlin Neutron Scattering Center, Helmholtz-Zentrum Berlin für Materialien und Energie, 14109 Berlin (Germany)
Dr. A. J. Ramirez-Cuesta
ISIS, Rutherford Appleton Laboratory, Oxfordshire (UK)

[**] This work was supported by an Australian Research Council Discovery Project Grant (C.J.K.), an Australian PhD Award, and Post-Graduate Research Awards (Y.W.) from the Australian Government and the Australian Institute of Nuclear Science and Engineering. ISIS facilities were accessed under the Major National Research Facilities Program.

Supporting information for this article is available on the WWW under http://dx.doi.org/10.1002/anie.200903366.

400 K, enabling comparison at the same temperatures with spectra calculated from ab initio molecular dynamics (MD) simulations. This is important because calculations involving an entire $[Cu_3(btc)_2]$ unit cell are beyond computing resources, and the validity of using the primitive cell approximation in the MD simulation needs to be determined. An abrupt step from a low-energy sub-minimum towards a slightly lower final minimum was noted during the energy-minimization procedure (required to obtain the starting structure for the MD simulation). This step is consistent with the bimodal characteristic of the structure discussed later.

The agreement between the simulated and measured INS spectra (Figure 2) is reasonable, and at 20 K is comparable to that obtained using finite displacements and normal-mode methods,[9] which used a primitive cell; such agreement arises from the local nature of the vibrations.

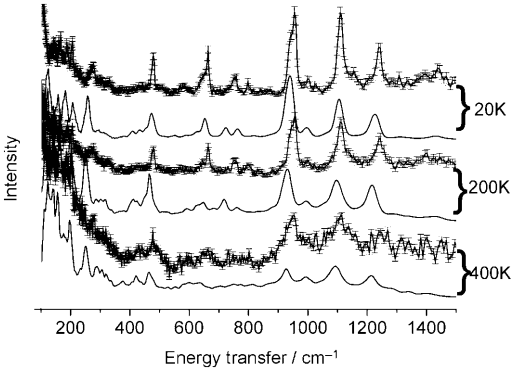

Figure 2. Temperature-dependent INS (neutron energy-loss) and calculated spectra from ab initio MD simulations in the energy range 100–1500 cm^{-1} for $[Cu_3(btc)_2]$ at 20, 200, and 400 K. Errors ($\pm$1 esd) are shown on the experimental spectra; all spectra are vertically displaced.

Low-energy INS spectra (20 and 100 K using a cold neutron time-of-flight instrument, Figure 3) show reasonable agreement with that calculated from the MD simulations,

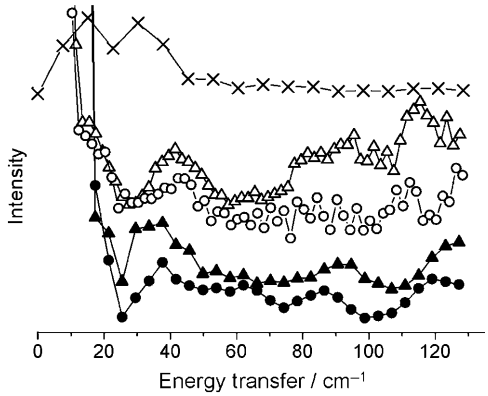

Figure 3. Low-energy INS spectra at 100 K (○ and ●) and 20 K (△ and ▲) for $[Cu_3(btc)_2]$. INS spectra are open symbols, and spectra calculated from the MD simulations are closed symbols (lower). The frequency spectrum (not transformed to neutron scattering)[10] of the paddlewheel torsion angle extracted from the MD trajectories at 60 K is shown at the top (×). Spectra are vertically displaced.

including the slight softening upon cooling of the features around 40 cm^{-1}. The experimental full $S(\mathbf{Q},\omega)$ surface shows no measurable dispersion for these features, indicating that they arise from local uncoupled modes; this is consistent with the ability of the primitive cell model to reproduce the measured spectra.

To investigate the vibrational origin of the low energy contributions below ca. 40 cm^{-1}, the frequency spectra of various framework fragments were extracted from the MD trajectories. The calculated spectrum of a paddlewheel mode (×, Figure 3), involving dynamic deformation of the square prismatic $\{Cu_2(carboxylate)_4\}$ paddlewheel units toward the square antiprismatic geometry with concerted rotation of the carboxylate groups and torsion about the Cu–Cu vector (see upper inset to Figure 1),[11] closely matches the phonon spectrum in this region. This shows that spectral features below 40 cm^{-1} contain contributions from motions that involve the deformation of this unit and, consequently, that paddlewheel vibration is an important NTE contributor.

A longer-range analysis of the MD trajectories reveals that despite correlation between intra-paddlewheel torsion angles corresponding to the concerted contra-rotation of rigid CuO_4 units, with correlation factor of 0.84, there is no clear correlation of this motion between neighboring paddlewheel units, with correlation factor 0.26 (see Supporting Information). This is consistent with the minimal dispersion in the INS data. This motion is strongly correlated, as expected, with the incumbent twist of the carboxylate unit about the benzene ring (correlation factor 0.79; Supporting Information, Figure S10).

As mapping the potential energy surface of the entire paddlewheel coordinate system is not feasible, even using the primitive cell, we approximated the system as a dicopper tetrabenzoate unit, $\{Cu_2(O_2C_7H_5)_4\}$, to explore the local dynamics. A MD simulation of this isolated unit using density functional theory (DFT, DMol^3)[12] shows the energy of the paddlewheel torsion at 60 K is ca. 20 cm^{-1}, approximately two-thirds that found in the periodic $[Cu_3(btc)_2]$ system. As differences in effective mass between the periodic system and the isolated unit would cause an energy shift in the alternate direction, these differences are attributed to a force constant effect, where the interactions of the paddlewheel torsion with the btc stiffen the unit, shifting vibrations to higher energies.

Mapping the potential energy of an isolated dinuclear Cu benzoate unit gives insight into the origin of the paddlewheel motions. The torsion angle was constrained to various angles in the range 0 to 10°, and all other atoms were free to move in the energy minimization. The relative energy of the torsion angle (□, Figure 4) is flatter than a simple cosine relationship (fitted between torsion angles of 0 and 45°) at angles below 10°. At 0° all levels are at least 4-fold degenerate due to spin and the $D_{4h}(4/mmm)$ local symmetry. As the torsion angle increases, the degenerate levels split, increasing the average energy for the majority of levels. The most notable exception is the 6th group of levels below the highest occupied molecular orbital (HOMO), which are deeper in the $D_{2h}(222)$ than for the $D_{4h}(4/mmm)$ conformation for a 10° torsion (Figures 4 and 5). The paddlewheel torsion allows one pair of these orbitals to distribute more evenly between the Cu and

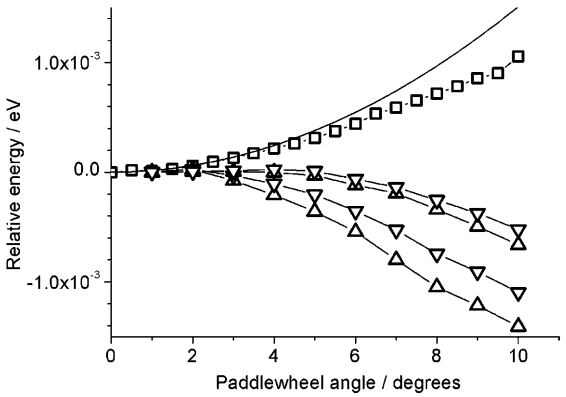

Figure 4. Paddlewheel torsion angle dependence of total energy (□) compared with a simple cosine potential (upper line). The four components of the 6th group of levels (see Figure 5) below the HOMO are also shown (△ and ▽). All calculations were made on an isolated dimeric Cu benzoate unit using spin unrestricted (not shown), spin-up (△), and spin-down (▽) calculations.

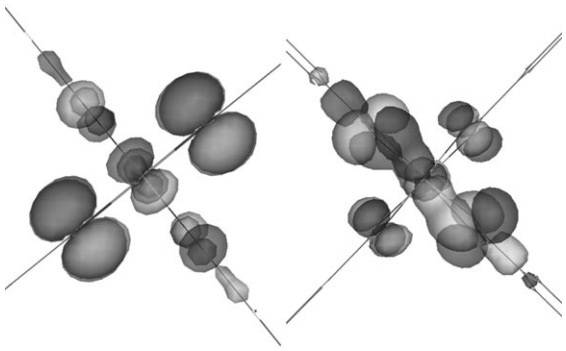

Figure 5. Undistorted (left) and distorted (right) dimeric Cu benzoate unit viewed down the Cu···Cu axis, with the paddlewheel torsion angle at 0° (left) and 10° (right). The orbitals correspond to the energy curves that are six levels below the HOMO and are associated with the two Cu and eight O atoms.

the btc units. The Cu···O distances in the minimum-energy structure are 1.9832 Å in the undistorted arrangement and 1.9818–1.9866 Å in the arrangement with a torsion angle of 10°. Hence, the interaction between the Cu and O atoms can be strengthened by the paddlewheel deformation.

A further feature of the MD trajectories is a bimodal distribution of paddlewheel torsion angles, with peaks corresponding to torsion angles approximately 4° on either side of the eclipsed conformation, the distribution increasing with temperature. The absence of an energy minimum at ca. 4°, determined from the MD simulation for the extended framework, indicates that the bimodal character arises from relief of framework strain inherent in the network topology, rather than from local electronic and/or steric effects. A high precision spin and symmetry-unrestricted ($P\bar{1}$ space group) energy minimization, starting from the symmetric primitive cell, resulted in a non-distorted square-planar unit. Minimization starting from a MD frame where the paddlewheel unit was distorted resulted in a structure with lower energy (24.3 kJ mol^{-1}). This structure featured a range of paddlewheel arrangements with torsion angles between 2.7 and 4.9°.

Confirming the tendency of the paddlewheel torsion angles to a bimodal distribution using diffraction methods is difficult due both to the overall distribution of paddlewheel torsion angles and to the subtlety of the predicted dynamic distortion, with the ca. 4° torsion predicted corresponding to only a ca. 0.14 Å splitting of the carboxylate O atom. Both the NPD (see Supporting Information) and previously reported SCXRD data[6] are insufficient to resolve any bimodal component present in the structure, with each being fitted adequately by isotropic and anisotropic refinement of a single O atom site, respectively. Inspection of the temperature-dependent anisotropic ADPs, however, reveal a zero-point extrapolation that is significantly larger than zero, consistent with there being a "dumbbell"-shaped component arising from dynamic displacement of the O atom, as predicted by the MD simulation. From the SCXRD data, the ADP in the direction of the predicted atom site splitting (see Supporting Information) intercepts 0 K at 0.011 Å^2, indicating a maximum possible root-mean-square O atom splitting of ca. 0.2 Å, depending on the extent of zero-point motion; this is consistent with the typical 0.15 Å splitting predicted by the MD simulations at 60 K. Similarly, the 0 K intercept of the isotropic ADPs for the O atom from the NPD refinements is 0.009 Å^2, again indicating a maximum splitting of ca. 0.2 Å. Using lattice dynamics[14] we calculate the zero-point motion of the O atom, close to isotropic at this point, to be 0.0044 Å^2. Our experimentally measured values are more than double this and consistent with our values from linear extrapolation.

To conclude, we show through crystallography, spectroscopy, and simulation that local molecular vibrations, in addition to concerted transverse vibrations, can contribute to NTE. This provides an entirely new approach for the achievement of anomalous thermal expansion. Specifically, our results indicate that the dinuclear Cu paddlewheel units within the metal–organic framework [$Cu_3(btc)_2$] have a broad potential energy curve, likely with two minima where the torsion angle is approximately 4° on either side of the eclipsed conformation due to relaxation of the framework's inherent geometric strain. We note that whilst the undistorted paddlewheel arrangement has the lowest overall energy for the isolated unit, some groups of energy levels are lower in a distorted conformation, resulting in a dinuclear node that undergoes NTE-inducing deformation at low energies. MD results show that the energy cost of the paddlewheel deformation is offset by the energy gain in the Cu–btc bonds, resulting in a soft anharmonic potential energy surface for the NTE mode.

Experimental Section

[$Cu_3(btc)_2$] was prepared hydrothermally;[6] deuterated btc was used for the preparation of the NPD sample, which was desolvated at 160 °C under dynamic high vacuum for 12 h.

INS data were collected on a 2.40 g sample of [$Cu_3(btc)_2$] for 8 h on TOSCA at the Rutherford Appleton Laboratory at 20, 100, 200, 300, and 400 K. Low-energy INS data were collected on a 0.915 g sample using NEAT at the Berlin Neutron Scattering Center. Incident neutrons at $\lambda = 2.1$ Å were used in an instrument configuration with 1.23 meV energy resolution at the elastic line. Spectra were collected

in neutron energy loss with a maximum neutron energy transfer of −16.07 meV. Data were collected for 8 h at 20 K and for 1 h at 100 K.

NPD data were collected for 4 h on a 0.52 g sample using Echidna at the OPAL Reactor, at 20, 40, 60, 100, 200, and 300 K. Full-structural Rietveld refinements were carried out using the GSAS[13] program as implemented in EXPGUI.[15]

Calculations on periodic cells were performed using VASP.[16] Energy minimizations used high-precision with spin-unrestricted calculations. MD simulations used low-precision electronic calculations. 1 fs time-steps were used and an initial thermalisation within canonical ensemble was made for 2 ps followed by microcanonical ensemble for 5 to 8 ps. PBE pseudopotentials and a single k-point were used. For the non-periodic system, DMol^3[12] was used with PBE pseudopotentials, spin-unrestricted, and high-precision. Neutron spectra were calculated using a combination of NMoldyn[17] to obtain $S(\mathbf{Q},\omega)$ and local algorithms to provide direct comparison with the experimental spectra.

Received: June 22, 2009
Revised: August 17, 2009
Published online: December 8, 2009

Keywords: coordination frameworks · metal–organic frameworks · microporous materials · neutron scattering · thermal expansion

[1] B. F. Abrahams, P. A. Jackson, R. Robson, *Angew. Chem.* **1998**, *110*, 2801; *Angew. Chem. Int. Ed.* **1998**, *37*, 2656; H. Li, M. Eddaoudi, M. O'Keeffe, O. M. Yaghi, *Nature* **1999**, *402*, 276; C. J. Kepert, M. J. Rosseinsky, *Chem. Commun.* **1999**, 375.

[2] S. Kitagawa, R. Kitaura, S. Noro, *Angew. Chem.* **2004**, *116*, 2388; *Angew. Chem. Int. Ed.* **2004**, *43*, 2334; G. Férey, C. Serre, *Chem. Soc. Rev.* **2009**, *38*, 1380; C. J. Kepert, *Chem. Commun.* **2006**, 695.

[3] F. Millange, C. Serre, N. Guillou, G. Ferey, R. I. Walton, *Angew. Chem.* **2008**, *120*, 4168; *Angew. Chem. Int. Ed.* **2008**, *47*, 4100; G. J. Halder, C. J. Kepert, *J. Am. Chem. Soc.* **2005**, *127*, 7891; J. P. Zhang, X. M. Chen, *J. Am. Chem. Soc.* **2008**, *130*, 6010.

[4] Y. Liu, J. H. Her, A. Dailly, A. J. Ramirez-Cuesta, D. A. Neumann, C. M. Brown, *J. Am. Chem. Soc.* **2008**, *130*, 11813; A. L. Goodwin, C. J. Kepert, *Phys. Rev. B* **2005**, *71*, 140301.

[5] A. E. Phillips, A. L. Goodwin, G. J. Halder, P. D. Southon, C. J. Kepert, *Angew. Chem.* **2008**, *120*, 1418; *Angew. Chem. Int. Ed.* **2008**, *47*, 1396; A. L. Goodwin, M. Calleja, M. J. Conterio, M. T. Dove, J. S. O. Evans, D. A. Keen, L. Peters, M. G. Tucker, *Science* **2008**, *319*, 794; A. L. Goodwin, D. A. Keen, M. G. Tucker, *Proc. Natl. Acad. Sci. USA* **2008**, *105*, 18708; A. L. Goodwin, B. J. Kennedy, C. J. Kepert, *J. Am. Chem. Soc.* **2009**, *131*, 6334; S. Margadonna, K. Prassides, A. N. Fitch, *J. Am. Chem. Soc.* **2004**, *126*, 15390.

[6] Y. Wu, A. Kobayashi, G. J. Halder, V. K. Peterson, K. W. Chapman, N. Lock, P. D. Southon, C. J. Kepert, *Angew. Chem.* **2008**, *120*, 9061; *Angew. Chem. Int. Ed.* **2008**, *47*, 8929.

[7] D. Dubbeldam, K. S. Walton, D. E. Ellis, R. Q. Snurr, *Angew. Chem.* **2007**, *119*, 4580; *Angew. Chem. Int. Ed.* **2007**, *46*, 4496; S. S. Han, W. A. Goddard, *J. Phys. Chem. C* **2007**, *111*, 15185; W. Zhou, H. Wu, T. Yildirim, J. R. Simpson, A. R. H. Walker, *Phys. Rev. B* **2008**, *78*, 054114.

[8] S. S.-Y. Chui, S. M.-F. Lo, J. P. H. Charmant, A. G. Orpen, I. D. Williams, *Science* **1999**, *283*, 1148.

[9] C. M. Brown, Y. Liu, T. Yildirim, V. K. Peterson, C. J. Kepert, *Nanotechnology* **2009**, *20*, 204025.

[10] Transformation from frequency and amplitude to the INS signal involves the momentum transfer, the neutron scattering cross section, attenuation factors, and instrumental resolution. This transformation has not been made. The frequency spectrum represents the Fourier-transform of the displacements from the time to the frequency domains only.

[11] The torsion about the Cu–Cu vector is defined as the dihedral angle formed by three vectors, O–Cu, Cu–Cu, and Cu–O (see Supporting Information). This angle is zero in the undistorted paddlewheel arrangement.

[12] B. Delley, *J. Chem. Phys.* **2000**, *113*, 7756.

[13] A. C. Larson, R. B. VonDreele, *Los Alamos Natl. Lab. Rep.* **2000**, *LAUR*, 86.

[14] K. Parlinski, PHONON (**2005**).

[15] B. H. Toby, *J. Appl. Crystallogr.* **2001**, *34*, 210.

[16] G. Kresse, J. Furthmüller, *Phys. Rev. B* **1996**, *54*, 11169.

[17] G. R. Kneller, V. Keiner, M. Kneller, M. Schiller, *Comput. Phys. Commun.* **1995**, *91*, 191.

